Carbohydrate Polymers 119 (2015) 159–166

Contents lists available at ScienceDirect

Carbohydrate Polymers

journal homepage: www.elsevier.com/locate/carbpol

Structure–property relationships of carboxymethyl hydroxypropyl guar gum in water and a hyperentanglement parameter

Daniel Szopinski, Werner-Michael Kulicke, Gerrit A. Luinstra*

Institute for Technical and Macromolecular Chemistry, University of Hamburg, Bundesstraße 45, 20146 Hamburg, Germany

ARTICLE INFO

Article history:
Received 1 October 2014
Received in revised form 27 October 2014
Accepted 21 November 2014
Available online 3 December 2014

Keywords:
Guar gum
CMHPG
Hyperentanglement
Steady state shear
Small amplitude oscillatory shear
Shear dependent viscosity

ABSTRACT

The viscoelastic properties of carboxymethyl hydroxypropyl guar gum (CMHPG) in aqueous solution were determined as function of concentration and of molecular weight, using SEC/MALLS/dRI and viscometry. The chain is more rigid as in native guar as was deduced from the molecular parameter in dilute solution. Superstructures are formed in moderately concentrated solutions as is shown from the comparison of steady state shear and small amplitude oscillatory shear (SAOS) experiments. The shear rate dependent viscosity of CMHPG can satisfactorily be described by the Carreau–Yasuda model with the rheological parameters (η_0, λ_0, n, b) obtained from the evaluation of viscosity data. A quantitative hyperentanglement parameter is introduced to account for the differences in responses in shear and SAOS experiments.

1. Introduction

Guar gum is a natural non-ionic polysaccharide from the endosperm of the guar bean (*cyamopsis tetragonoloba*), which primarily grows in India and Pakistan. The water-soluble galactomannan has a linear backbone of β-1,4 linked D-mannopyranosyl units and randomly, in pairs and triplets arranged α-1,6 linked D-galactopyranosyl units as side chains (Dea & Morrison, 1975; Hoffman & Svensson, 1978; McCleary, Clark, Dea, & Rees, 1985). The mannose to galactose ratio typically ranges between 1.6 and 1.8 and is dependent on the natural source (Cheng, Brown, & Prud'homme, 2002). Guar gum is used in food, agriculture, pharmaceutical and textile applications, and, also for technical purposes like hydraulic fracturing (Cheng & Prud'homme, 2000; Tayal, Pai, & Khan, 1999; Tizzotti et al., 2010). The high viscosity of aqueous solutions at low concentrations is the main driver for guar gum application, which results from the high molecular weight (1000–2000 kg mol^{-1} (Vijayendran & Bone, 1984)) and the segment-segment interactions of the unbranched parts of the backbone, the so called *"hyperentanglements"* (Goycoolea, Morris, & Gidley, 1995; Morris, Cutler, Ross-Murphy, Ress, & Price, 1981; Wientjes, Duits, Jongschaap, & Mellema, 2000). The latter interactions are part of discussions, in particular with respect to the importance in aggregated particles and for the state of hydration of the guar gum (Picout, Ross-Murphy, Errington, & Harding, 2001).

Guar gum may chemically be modified to increase the ease of handling, in particular the dissolution in water. Commercial available derivatives thus may contain hydroxypropyl (HP) and/or carboxymethyl (CM) groups. These derivatives have enhanced thermal stability, hydration properties and generally contain fewer insoluble parts as the parent polysaccharide. HPG, CMG and CMHPG are claimed in patents as additives for fracturing fluids in mining and mineral industry and oil recovery operations (Banerjee et al., 2009; Kesevan & Prud'homme, 1992; Lapasin, De Lorenzi, Pricl, & Torriano, 1995; Lei & Clark, 2007; Zhang & Zhou, 2006). The rheological behavior of the HP and/or CM derivatives has not comprehensively been reported upon and is of more than academic interest (Risica, Barbetta, Vishetti, Cametti, & Dentini, 2010). In fact, only a few studies of carboxymethyl hydroxylpropyl guar gum (CMHPG, Fig. 1) are available (Bahamdan & Daly, 2007; Lei & Clark, 2007; Mukherjee, Sarkar, & Moulik, 2010; Pasha & Ngn, 2008; Shi & Zhang, 2007; Zhang, Zhou, & Hui, 2005; Zhang & Zhou, 2006). The aim of the current study is to increase the understanding of the complex solution structures and to extend the knowledge on the flow behavior in more concentrated solutions.

The five states of polymer solution introduced by Graessley, Hazelton, and Lindeman (1967) were used to describe the behavior of CMHPG in solution, i.e. (1) ideally dilute particle solution, (2) semi-dilute particle solution, (3) semi-dilute network solution, (4) concentrated particle solution and (5) concentrated network solution. The shear rate dependent viscosity of a polymer solution

* Corresponding author. Tel.: +49 0 40 42838 3162; fax: +49 0 40 42838 6008.
E-mail address: luinstra@chemie.uni-hamburg.de (G.A. Luinstra).

http://dx.doi.org/10.1016/j.carbpol.2014.11.050
0144-8617/

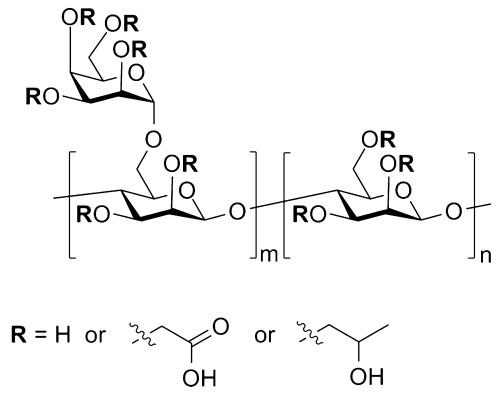

Fig. 1. Generic structure of carboxymethyl hydroxypropyl guar gum (CMHPG).

can accordingly be characterized by three parameters: the zero-shear viscosity η_0 in the Newtonian region at low shear rates, the slope n in the Non-Newtonian region at high shear rates and the longest relaxation time λ_0 as a measure for the transition between the latter regions. The technical application of guar gum derivatives is in the regime between semi-dilute particle solution and semi-dilute network solution. The establishment of empirical structure–property relationships would allow the determination of η_0, λ_0 and n as functions of the overlap parameter $c \times [\eta]$. The shear-dependent viscosity at the various states of solution with respect to molecular parameters may then be predicted with reasonable accuracy.

Additionally, insight was obtained into the nature of the solution structures. A master curve was constructed for concentrated solutions by plotting the zero-shear viscosity η_0 against the product of concentration and weight average molecular weight, $c \times M_w$ (Büche, 1952). For more dilute solutions, the normalization by $c \times M_w$ is not sufficient to describe the behavior and the influence of the solvent by polymer coil expansion was taken into account. Simha and Zakin (1962) proposed the description of the zero-shear viscosity η_0 in semi-dilute solutions as a function of the overlap parameter $c \times [\eta]$. This approach was followed to obtain linear structure-property relationships. Fig. 2 outlines the states of solution in dependence of concentration and molecular weight.

2. Materials and methods

2.1. Materials

Carboxymethyl hydroxypropyl guar gum ($M_W = 1360\ kg\ mol^{-1}$) with typical degrees of substitution in industrial applications ($DS_{Gal} = 0.54$, $DS_{CM} = 0.06$, $MS_{HP} = 0.25$) was used. This kind of derivative is easily prepared from native guar gum (Pasha & Ngn, 2008; Venkataiah & Mahadevan, 1982). The dry weight and insoluble residues were detemined and considered in the sample preparation. Sodium nitrate (ReagentPlus, ≥99.0%) and sodium azide (ReagentPlus, ≥99.5%) were purchased from Sigma-Aldrich Chemicals and used as received. 0.1 M $NaNO_3$ + 200 ppm NaN_3 was used as solvent to minimize the "polyelectrolyte effect" and to inhibit bacterial degradation of the polysaccharide. Ultrasonic degradation was carried out with a Branson 450 sonifier with a 3/4″ titanium resonator operated at a frequency of 20 kHz (duty cycle: 50%, power output: 1–10, $T = 278.15$ K). CMHPG solutions (0.5 wt%) were prepared in demineralized water and lyophilized after ultrasonification. Titanium dust originating from the sonifier was removed with an ultracentrifuge (30 min, 7000 g).

2.2. Characterization

2.2.1. NMR spectroscopy

^1H NMR and ^{13}C-IGATED spectra of CMHPG were recorded using a Bruker AVANCE 400 MHz spectrometer. Samples were dissolved in D_2O, data collection was at 343 K. The average degree of substitution of D-galactopyranosyl units ($DS_{Gal} = 0.54$), carboxymethyl groups ($DS_{CM} = 0.06$) and molar degree of substitutions of hydroxypropyl groups ($MS_{HP} = 0.25$) were determined by integration of the corresponding signals (for details, see Supporting material).

2.2.2. Viscometry

Measurements were carried out in an micro-Ubbelohde capillary viscometer (Type 1c, Schott, Germany) at 25 °C in water

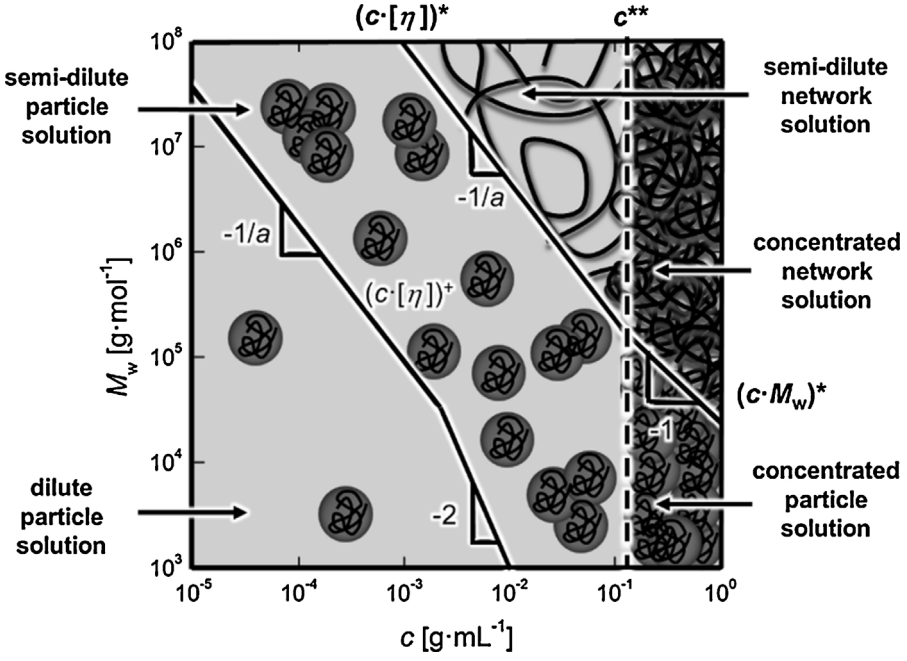

Fig. 2. Outline of the five states of solution (redrawn with permission from Clasen & Kulicke, 2001).

Table 1
Data of degraded CMHPG.

Power output	t [min]	M_W/M_n [kg mol^{-1}]	$[\eta]$ [mL g^{-1}]	K_H	$c_\eta*$ [mg mL^{-1}]	$\langle R_G^2\rangle_z^{0.5}$ [nm]	$c_{LS}*$ [mg mL^{-1}]
–	–	1360/1200	1599	0.579	1.6	109.6	0.41
2	0.5	1160/933	1290	0.934	1.9	101.8	0.44
5	0.5	828/741	1095	1.351	2.3	94.6	0.39
3	4	620/372	910	0.584	2.7	83.4	0.42
3	8	492/384	740	0.463	3.4	61.9	0.82
3	12	429/358	693	0.108	3.6	57.3	0.91

intrinsic viscosity $[\eta]$, Huggins coefficient K_H, overlap concentration from viscosimetry $c_\eta*$, overlap concentration $c_{LS}*$ from MALLS.

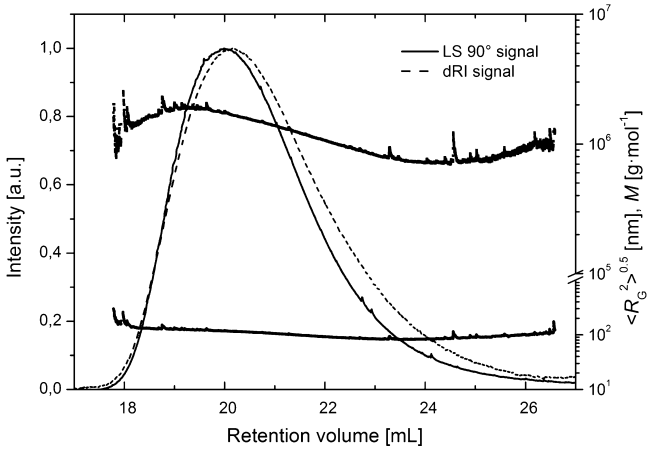

Fig. 3. Elugram of CMHPG of M_W = 1190 kg mol^{-1} showing the signal originating from the scattered light and of the refractive index detector next to the derived root mean square radius of gyration and the molecular weight M_W (V = 0.5 ml min^{-1}, T = 298.15 K, 0.1 M $NaNO_3$ + 200 ppm NaN_3).

having a $NaNO_3$ concentration of 0.1 M and containing 200 ppm NaN_3. The intrinsic viscosity $[\eta]$ was calculated according to $[\eta] = \lim_{\substack{c\to 0\\ \dot\gamma\to 0}} \eta_{red}$, where η_{red} is the concentration dependent reduced viscosity (Kulicke & Clasen, 2004).

2.2.3. Rheometry

Rheological measurements were performed on AR 2000 ex and G2 controlled stress rheometers (TA Instruments, New Castle, USA) with a cone-plate geometry (diameter = 60 mm, angle = 2°). SAOS experiments were carried out at a frequency range of 0.1 to 100 rad s^{-1}. The strain (γ_0 = 1–10%) was kept within the limits of the linear viscoelastic regime at a temperature of 298.15 K.

2.2.4. SEC/MALLS/dRI

The molecular weight and root mean square radius of gyration were determined by size exclusion chromatography (precolumn and two columns 10,000 Å, 20 μm, 8.0 × 300 mm, PSS Suprema, Mainz, Germany) coupled to a multiangle laser light scattering detector (DAWN-EOS, Wyatt Technology Corp., Santa Barbara, USA) and a refractive index detector (Optilab rEX, Wyatt). A typical elugram is shown in Fig. 3.

3. Results and discussion

3.1. Chain conformation and flexibility in dilute solution

The molecular structure, coil size and conformation and the chain flexibility of CMHPG are parameters that significantly determine the flow behavior of its aqueous solutions. Insights can be reached by characterizing a homologous series of molecular weights with respect to intrinsic viscosity and radius of gyration. Ultrasonic degradation of CMHPG gave access to CMHPGs with molecular masses M_W ranging from about 429 to 1360 kg mol^{-1}. A significant advantage of this method is the preservation of the chemical composition along the chain, and the prevention of reactions occurring at the side chain (substituents) (Kulicke, Otto, & Baar 1993; Baar, Kulicke, Szablikowski, & Kiesewetter, 1994). The weight- and number-average molecular weight M_W/M_n and the z-average radius of gyration $\langle R_G^2\rangle_z^{0.5}$ were calculated from SEC/MALLS/dRI combined analytics. The corresponding critical overlap concentrations for selected samples were derived (Table 1).

Capillary viscosimetric experiments on CMHPGs in dilute solutions (Fig. 4a) show the expected linear relation of the polymer concentration c and the reduced viscosity η_{red} in a Huggins plot. The Huggins constant K_H ranges from 0.108 to 1.351 illustrating that the solvation quality decreases with molecular weight. They are in the range reported for guar gum (Ma & Pawlik, 2007). The intrinsic viscosity $[\eta]$ as function of the molecular weight follows the Kuhn–Mark–Houwink–Sakurada (KMHS) relationship $[\eta] = K_a \times M_w^a$ with K_a = 0.085 and a = 0.69 (±0.04) (Fig. 4b). The latter value shows that CMHPG behaves as a partially expanded coil in the solvent. The value is close to that found for native guar gum (a = 0.70–0.75) (Beer, Wood, & Weisz, 1999; Cheng et al., 2002; Picout et al., 2001; Robinson, Ross-Murphy, & Morris 1982) and methylated guar gum (a = 0.73–0.76, DS_M = 0.3–0.6) (Risica, Dentini, & Crescenzi, 2005). Hydroxylpropyl guar gum has a somewhat higher exponent a of 0.78 (MS_{HP} = 0.6) (Cheng et al., 2002).

The value of a of the CMHPG samples may be explained by a steric interactions of the side chains. The samples having a relatively low degree of substitution are comparable to the methylated guar gum studied by Risica. They noted that the exponent a increased with the degree of substitution, which was interpreted as a result of fewer hydrogen bonds (Risica et al., 2005). An increase in molecular volume has been put by Cheng to explain the even higher value of a for HPG, however this holds for HPG with high MS values. The intrinsic viscosity is smaller for HPG with lower MS values and is explained by reduced intermolecular interactions, which is the dominant effect at MS values up to 0.4 (Cheng et al., 2002).

The coil expansion in dilute solution may also be derived from an analysis along the Fox and Flory theory, which relates the intrinsic viscosity $[\eta]$ to the radius of gyration $\langle R_G^2\rangle_z^{0.5}$ and the weight-average molecular weight M_W (Eq. (1)). Knowledge of the interdependence of $\langle R_G^2\rangle_z^{0.5}$ and M_W reduces the equation to a one parameter expression (Eq. (1)) with K_ν and ν as constants from the $\langle R_G^2\rangle_z^{0.5} - M_w$ relationship and Φ as the Flory constant).

$$[\eta] = \Phi \times \frac{\langle R_G^2\rangle_z^{1.5}}{M_w} = \Phi \times {K_\nu}^3 \times M_w^{3\nu-1} \quad (1)$$

The $\langle R_G^2\rangle_z^{0.5} - M_W$ relationship was deduced from light scattering data, Fig. 5 shows the corresponding double logarithmic plot. The numerical evaluation of the linear part yields to $\langle R_G^2\rangle_z^{0.5} = 0.036 \times {M_w}^{0.56}$. The Flory constant Φ of the system is

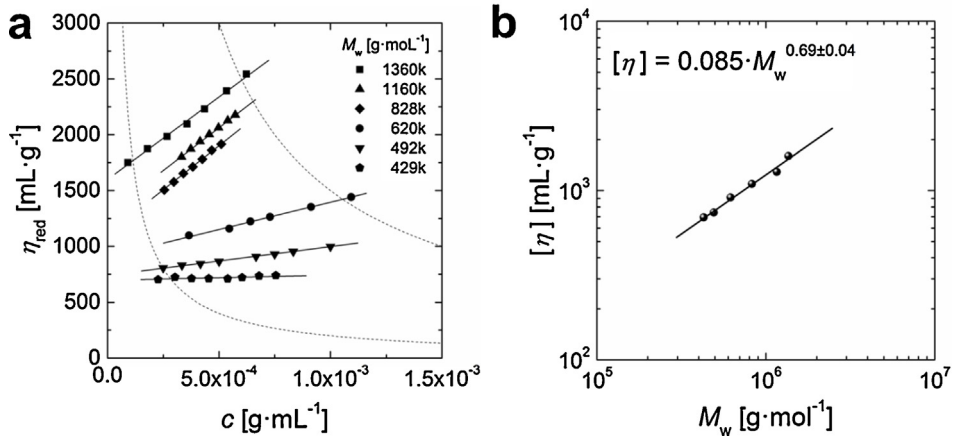

Fig. 4. (a) Huggins plot for CMHPG with various weight average molecular weights M_W. The dashed lines represent the range of relative viscosity η_r between 1.2 and 2.5 (b) double logarithmic Kuhn–Mark–Houwink–Sakurada plot in water (0.1 M $NaNO_3$, 200 ppm NaN_3; T = 25 °C).

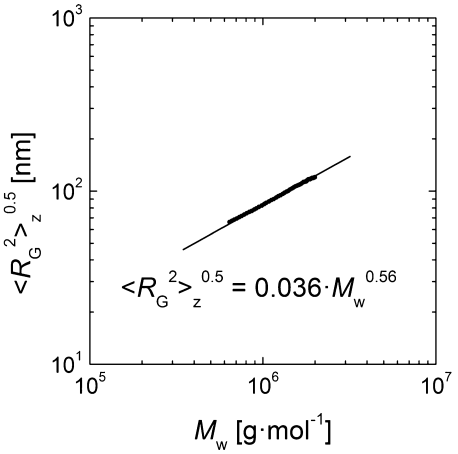

Fig. 5. The z-average root mean square radius of gyration $\left\langle R_G^2 \right\rangle_z^{0.5}$ as a function of M_W for a series of ultrasonic degraded CMHPG.

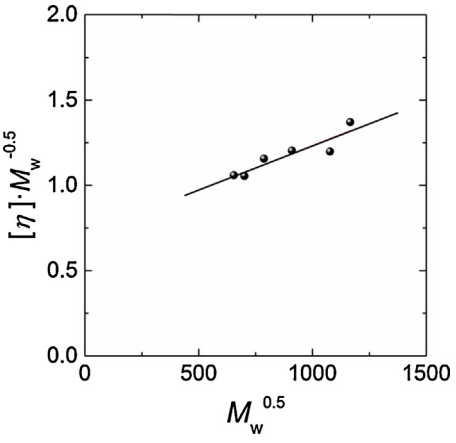

Fig. 6. Burchard–Stockmeyer–Fixman plot for CMHPG dissolved in 0.1 M $NaNO_3$ + 200 ppm NaN_3 (T = 298.15 K).

approximated according to $\Phi = \Phi_\theta \left(1 - 2.63\varepsilon + 2.86\varepsilon^2\right)$, where Φ_θ is taken as $\Phi_\theta = 2.10 \times 10^{24}$ mol^{-1} for polyelectrolytes (Flory & Fox, 1951; Thielking & Kulicke, 1996; Yamakawa, 1971) and the correction for non-θ systems was applied with $\varepsilon = 2\nu - 1$, resulting in $[\eta]_{\text{Fox–Flory}} = 0.071 \times M_w^{0.68}$. The exponential factor relating M_w to the intrinsic viscosity is basically equal to the one obtained from viscosimetric data, showing that coil expansion is described satisfactory. The preexponentional constants K = 0.085 and K = 0.071 differ to some extent, which is not unusual as different physical phenomena are underlying the analysis and in addition, Φ_θ may be too low for a system that is not a typical polyelectrolyte.

The intrinsic chain flexibility of CMHPG can be estimated following the analysis based on the Burchard–Stockmeyer–Fixman equation (Stockmayer & Fixman, 1963), $[\eta] \times M_w^{-0.5} = K_{a,\theta} + 0.51 \times \Phi B M_w^{0.5}$, where $K_{a,\theta}$ is the constant of the $[\eta] - M_w$ relationship at θ-conditions and $0.51 \times \Phi B$ is a measure of the long-range interactions. The constant $K_{a,\theta}$ is correlated to the characteristic ratio C_∞ by the equation $K_{a,\theta} = \Phi \times l^3 \times \left(C_\infty / m_0\right)^{-1.5}$, where l (= 0.54 nm) is the length and m_0 (= 279.45 g/mol) the average molecular weight of an anhydromannose unit with side chains in the CMHPG (DS_{Gal} = 0.54, DS_{CM} = 0.06, MS_{HP} = 0.25). The characteristic ratio C_∞ is a measure for the chain rigidity and coil expansion. It leads to the persistent length l_p when assuming a wormlike chain through the equation $C_\infty = 2 \times l_p \times l^{-1}$. Values of C_∞ = 23.2 (±1.2) and I_P = 6.3 (±0.3) nm were obtained. Compared to the reported values of native guar gum with C_∞ of 12.4–14.7 and l_p of 3.3–4.0 nm (Cheng et al., 2002; Picout et al., 2001; Robinson et al., 1982; Risica et al., 2005), CMHPG thus has a more rigid chain, plausibly originating from the steric crowding inflicted by the hydroxypropyl and the electronic repulsion of the partly charged carboxymethyl groups. Cheng et al. (2002) observed also a higher chain rigidity of HPG in comparison to native guar gum. Our study thus completes these insights into the coil dimensions and chain mobility in guar gum derivatives (Fig. 6).

3.2. Prediction of the flow behavior of CMHPG in steady state shear flow

The flow behavior of CMHPG in shear fields is relevant for many applications. The flow behavior of polymer solutions is dependent on the concentration and molecular weight. The modified Carreau–Yasuda model (Yasuda, Armstrong, & Cohen, 1981) was used here to describe the shear rate dependent viscosity of CMHPG solutions:

$$\eta(\dot{\gamma}) = \eta_\infty + (\eta_0 - \eta_\infty)\left[1 + (\lambda_0 \times \dot{\gamma})^b\right]^{n/b} \quad (2)$$

The model parameters are the zero-shear viscosity η_0, the infinite-shear viscosity η_∞, the longest relaxation time λ_0 and the slope n in the non-Newtonian region of the power law, describing the apparent viscosity as function of the shear rate. The independent determination of these parameters is possible from several

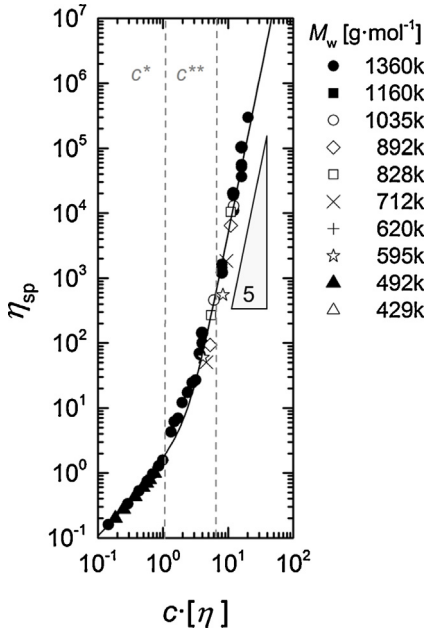

Fig. 7. Specific viscosity η_{sp} as a function of the overlap parameter $c \times [\eta]$ for CMHPG dissolved in 0.1 M $NaNO_3$ + 200 ppm NaN_3 (T = 298.15 K).

structure–property relationships interlinking viscosity, concentration and molecular weight or coil dimensions. The transition parameter b describes the width of the transition region between Newtonian and non-Newtonian behavior, and is usually fitted. The infinite-shear viscosity η_∞ is difficult to measure and is often set to $\eta_\infty = 0$ für aqueous solution (Yasuda, 2006).

The zero-shear viscosity η_0 of a polymer solution may be described on basis of the overlap parameter $c \times [\eta]$, which comprise contributions of the molecular weight, concentration and the solvent-polymer interactions. The specific viscosity η_{sp} ($= (\eta_0 - \eta_s) \times \eta_s^{-1}$, with η_s being the viscosity of the solvent) of CMHPG can be fitted to a master curve as a function of the overlap parameter $c \times [\eta]$ along Eq. (3) (Kulicke & Klare, 1980; Kulicke, Kniewske, Müller, Prescher, & Kehler, 1986). This approach corresponds to an extended Huggins virial equation, which also takes the polymer interactions at higher concentrations into account. The additional power term $B_n(c \times [\eta])^n$ is sufficient to describe the increase of the specific viscosity η_{sp} in moderately concentrated solutions and was determined by linear regression at high overlap parameters in the state of semi-dilute network solution shown in Fig. 7.

$$\eta_{sp} = c \times [\eta] + K_H(c \times [\eta])^2 + B_n(c \times [\eta])^n \quad \text{with} \quad n = \frac{3.4}{a} \tag{3}$$

The relationship for CMHPG thus reads

$$\eta_{sp} = c \times [\eta] + (0.67 \pm 0.39) \times (c \times [\eta])^2 + (5.43 \pm 0.80) \times 10^{-2} \times (c \times [\eta])^{4.98 \pm 0.19} \tag{4}$$

The exponent a of the $[\eta] - M_w$ relationship can alternatively be calculated from the exponent n of Eq. (3) to give a value for a of 0.68, which is in good agreement with the value from viscosimetry (Kulicke & Kniewske, 1984). The zero-shear rate viscosity η_0 may accordingly be obtained from Eq. (5) taking into account that $\eta_{sp} = (\eta_0 - \eta_s) \times \eta_s^{-1}$, with η_s being the viscosity of the solvent.

$$\eta_0 = \eta_s \left(c \times [\eta] + (0.67 \pm 0.39) \times (c \times [\eta])^2 + (5.43 \pm 0.80) \times (c \times [\eta])^{4.98 \pm 0.19} + 1\right) \tag{5}$$

The transition between semi-dilute particle solution and semi-dilute network solution is correspondingly at $c* \sim 1.1 \times [\eta]^{-1}$ and the transition to a concentrated network solution at $c** \sim 6.6 \times [\eta]^{-1}$ (dashed lines in Fig. 7). These low critical overlap concentrations demonstrate the water-thickening potential of CMHPG compared to analogous polysaccharides generating highly viscous solutions (Storz, Zimmermann, Zimmermann, & Kulicke, 2010).

Kulicke et al. (1986) suggested to relate the longest relaxation time λ_0 to the overlap parameter $c \times [\eta]$ along Eq. (6). The values for λ_0 measure the onset of the non-Newtonian region and are the reciprocal of the critical shear rate $\dot{\gamma}_c$.

$$\lambda_0 = K_\lambda \times c^{-(1+1/a)} \left((c \times [\eta])^2 + K_H(c \times [\eta])^3 + B_n(c \times [\eta])^{n+1}\right) \tag{6}$$

Following this approach, a linear correlation between $\lambda_0 \times c^{(1+1/a)}$ and the overlap parameter was found, setting a to 0.69 (Fig. 8). Numerical evaluation leads to the expression in Eq. (7), where $K_\lambda = 3.7 \times 10^{-11}$.

$$\lambda_0 = (3.7 \pm 0.2) \times 10^{-11} \times c^{-(1+1/0.69)} \left((c \times [\eta])^2 + (0.67 \pm 0.39) \times (c \times [\eta])^3 + (5.43 \pm 0.80) \times 10^{-2} \times (c \times [\eta])^{5.98}\right) \tag{7}$$

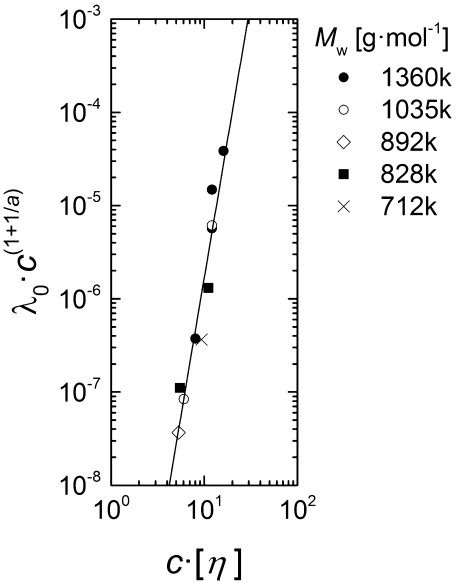

Fig. 8. Product of $\lambda_0 \cdot c^{(1+1/a)}$ as a function of the overlap parameter $c \times [\eta]$ for CMHPG dissolved in 0.1 M $NaNO_3$ + 200 ppm NaN_3 (T = 298.15 K).

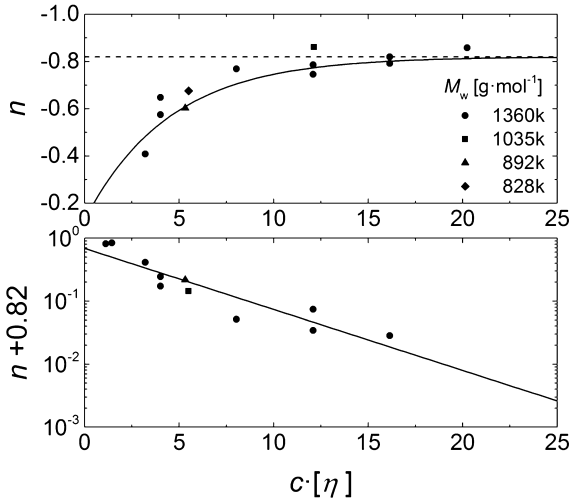

Fig. 9. Slope η as a function of the overlap parameter $c \times [\eta]$ for CMHPG dissolved in 0.1 M $NaNO_3$ + 200 ppm NaN_3 (T = 298.15 K).

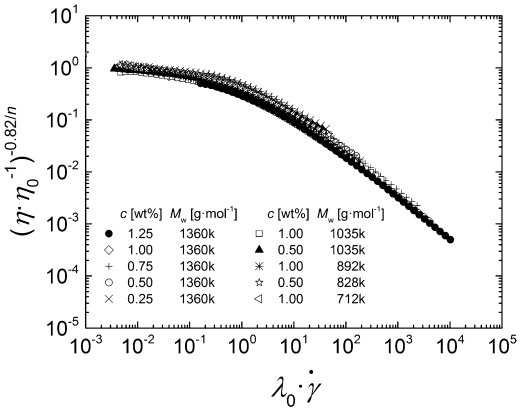

Fig. 10. The reduced shear viscosity $\left(\eta \times \eta_0^{-1}\right)^{-0.82/n}$ as a function of the reduced shear rate $\lambda_0 \cdot \gamma$ for different molecular weights and concentrations in 0.1 M $NaNO_3$ + 200 ppm NaN_3 (T = 298.15 K).

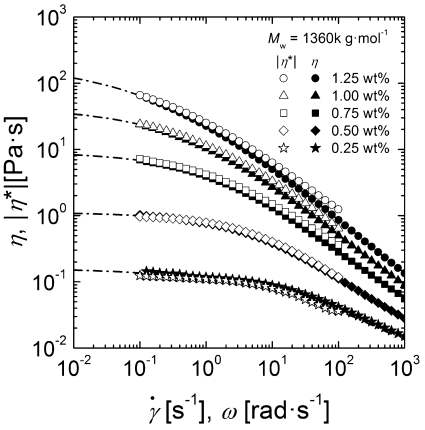

Fig. 12. Shear viscosity η as a function of shear rate γ and the magnitude of the oscillation viscosity $|\eta^*|$ as a function of angular frequency ω for CMHPG (Cox–Merz rule) at different concentrations in 0.1 M $NaNO_3$ + 200 ppm NaN_3 (T = 298.15 K). The dash dotted line is the Carreau–Yasuda model approximation.

Graessley et al. (1967) derived a theoretical slope of $n = -0.82$ for the dynamic viscosity as function of the shear rate in the non-Newtonian region of concentrated solutions and polymer melts. This presumption does not necessarily hold in semi-dilute solutions, as was observed for the solutions used of CMHPG. Bouldin and Kulicke rather used the overlap parameter $c \times [\eta]$ to account for the differences in more dilute solutions along Eq. (8) (Bouldin, Kulicke, & Kehler, 1988).

$$n = -0.82 + k_{n,1} \times 10^{k_{n,2} \times c \times [\eta]} \tag{8}$$

Indeed, a semi-logarithmic plot of $\log(n + 0.82) = \log k_{n,1} + k_{n,2} \times c \times [\eta]$ is linear (Fig. 9) and allows the determination of the constants to yield the $n - [\eta] - c$ relationship for CMHPG:

$$n = -0.82 + (0.69 \pm 0.45) \times 10^{(-0.097 \pm 0.013) \times c \times [\eta]} \tag{9}$$

The now established structure–property relationships for the zero-shear viscosity η_0, the longest relaxation time λ_0 and the slope n in the non-Newtonian region allows the prediction and calculation of the shear rate-dependent viscosity with respect to the molecular weight and concentration by inserting them into the Carreau–Yasuda model (Eq. (2)). The transition parameter b, is found by fitting the experimental steady state shear flow data to the model. The variation of the transition parameter with respect to concentration and molecular weight can be evaluated by plotting master curves encompassing solutions of CMHPG at various concentrations and molecular weights (Fig. 10). The transition parameter b for CMHPG varies between 0.30 and 0.71 and on average is 0.57 ± 0.12.

3.3. Hyperentanglements and the first normal stress difference N_1

Recently, Sharma and McKinley (2012) introduced a further empirical rule for calculating the first normal stress difference N_1 from the steady state flow (Eq. (10), the AbNormal rule). Two lesser known Cox–Merz rules were combined with the well-known Laun rule (Eq. (11)) to arrive at Eq. (10) that allows the calculation of N_1 at lower shear rates. It was shown, that the equation may yield N_1 with an accuracy that is higher than of the Laun rule.

$$N_{1,\ \text{Abnormal}}(\dot{\gamma}) \cong 2\dot{\gamma}\eta\left(1 - \frac{\eta_c^2}{\eta^2}\right)^{0.5}\left(\frac{\eta_c^2}{\eta^2}\right)^{-0.7} \tag{10}$$

$$N_{1,\text{Laun}}(\dot{\gamma})\big|_{\omega=\dot{\gamma}} \cong 2G'(\omega)\left(1 + \left(\frac{G'(\omega)}{G''(\omega)}\right)^2\right)^{0.7} \tag{11}$$

This approach was verified for CMHPG solutions. The measured first normal stress difference N_1 is therefore compared to the calculated first normal stress differences from the AbNormal and Laun rule (Fig. 11). It is evident from visual inspection that the Abnormal rule overestimates the normal stress difference, although the

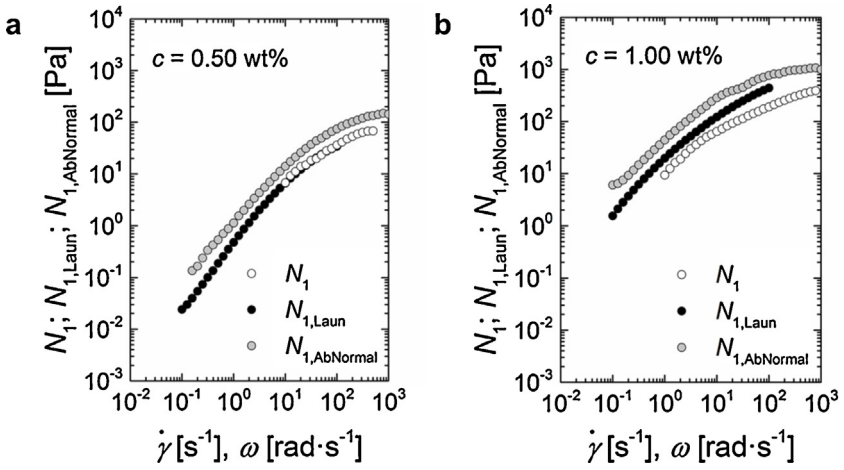

Fig. 11. Measured first normal stress difference N_1 and calculated normal stress differences $N_{1,\text{Laun}}$ and $N_{1,\text{Abnormal}}$ as a function of shear rate γ or of angular frequency ω for CMHPG (M_W = 1360 kg mol^{-1}) at a concentration of (a) c = 0.50 wt% and (b) c = 1.00 wt% in 0.1 M $NaNO_3$ + 200 ppm NaN_3 (T = 298.15 K).

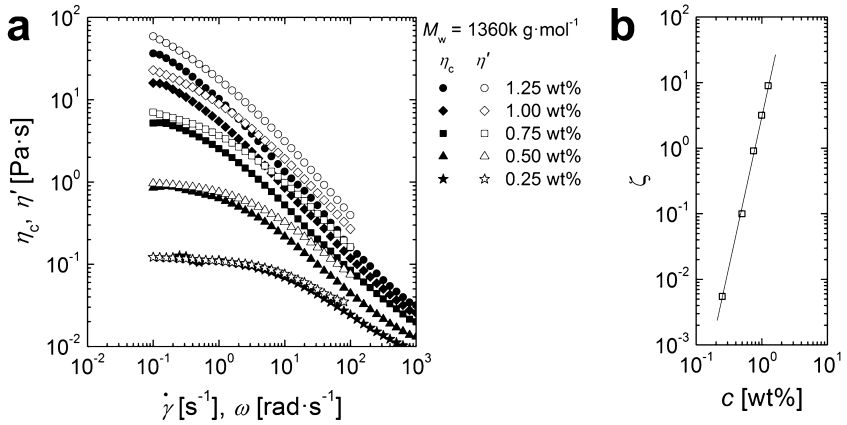

Fig. 13. (a) Consistency η_c as a function of shear rate γ and the real part of the complex oscillation viscosity η' as a function of angular frequency ω for CMHPG at different concentrations (b) Hyperentanglement parameter ξ as a function of concentration c in 0.1 M $NaNO_3$ + 200 ppm NaN_3 (T = 298.15 K).

frequency dependence is more or less well-described. The Laun rule gives an almost perfect match at a concentration of 0.5 wt%. At a higher concentration of 1 wt% the fits exceedingly deviate from the experimental values. This may be caused by the existence of superstructures ("hyperentanglements") in the solution that become of more than linear importance at higher concentrations.

3.4. Correlation between steady state shear flow and oscillatory shear flow

The fundamental empirical relations of the AbNormal rule were investigated for CMHPG solutions to introduce a measure for the hyperentanglements. The steady state shear viscosity η and the complex oscillation viscosity $|\eta*|$ may be equal for $\dot{\gamma} = \omega$ as was observed by Cox and Merz (1958), when the system is rheologically simple. This relationship is known as the Cox–Merz rule:

$$|\eta*(\omega)| \equiv \eta(\dot{\gamma})|_{\dot{\gamma}=\omega} \tag{12}$$

The viscosity of CMHPG solutions closely follows the Cox–Merz relationship at low concentrations and starts to deviate from it at higher concentrations of $c > 0.5$ wt% in the region of higher shear rates (Fig. 12). The existence of superstructures ("hyperentanglements") in the solution is the usual explanation put forward to account for it. In steady state shear flow the superstructures are dissolved during the measurement, whereas in SAOS these structures are preserved.

A further and more sensitive description of the difference between steady state shear flow and SAOS can be achieved by the application of a lesser known Cox-Merz rule from the same publication (Cox & Merz, 1958; Sharma & McKinley, 2012), as was recently elaborated by McKinley (Eq. (13)). This empirical relationship correlates the real part of the complex oscillation viscosity η' with the transient viscosity η_c, also known as consistency (Sharma & McKinley, 2012).

$$|\eta'(\omega)| \cong \eta_c(\dot{\gamma})|_{\dot{\gamma}=\omega} \quad \text{with} \quad \eta_c(\dot{\gamma}) = \frac{\partial \sigma_{12}}{\partial \dot{\gamma}} \tag{13}$$

The region of onset of shear thinning is of interest as entanglements and chain dragging interactions are being dissolved that cannot relax on the time scale of the action. The magnitude of shear thinning as function of the concentration may thus contain quantitative information on the interactions that are released.

The viscosity in steady state flow shear and SAOS measurements starts to derivate at higher concentrations of $c > 0.25$ wt% in the region of higher shear rates, indicative of a higher concentration of hyperentanglements (Fig. 13). Congruent to the analysis of the normal stress differences by Sharma, we suggest to introduce an hyperentanglement parameter ζ as the average of the differences in η' and transient viscosity η_c. This parameter can serve as a measure for the contribution of superstructures in CMHPG to the (shear dependent) viscosity.

$$\zeta = \left(\frac{1}{k} \sum_{i=1}^{k} \left(\eta_i' - \eta_{c,i} \right)^2 \right)^{0.5} \tag{14}$$

The hyperentanglement parameter ζ as a function of concentration is shown in Fig. 12b. It appears to follow a power law of $\zeta \propto c^{4.6}$ in the concentration range of 0.25 and 1.25 wt% and thus strongly depends on concentration. Future work will deal with the introduced hyperentanglement parameter ζ as a correction factor.

4. Concluding remarks

The fundament parameter of carboxymethyl hydroxylpropyl guar gum were determined from a combination of viscosimetric, rheological and scattering measurements. It forms a solid base to predict the (flow) behavior in aqueous solution. The chain conformation and flexibility of functionalized guar gums was determined in dilute solution comprising the KMHS constants K_a, a, the characteristic ratio C_∞ and the persistent length l_p. The data are indicative of a more rigid chain for CMHPG than of native guar gum. The shear dependent flow behavior of CMHPG solutions in steady state shear can be satisfactory described with the Carreau–Yasuda model, the variables η_0, λ_0 and n can be derived from the concentration and molecular weight, respectively, the intrinsic viscosity using the structure property relationships of the overlap parameter $c \times [\eta]$. The importance of hyperentanglements is evident at the calculation of the first normal stress difference N_1 from Laun's rule and the 2012 established rule by Sharma and McKinley. The introduction of an hyperentanglement parameter ζ as measure for superstructures and description of the discrepancy between steady state shear and SAOS was put forward.

Supplementary material

Details on the characterization of the samples by NMR.

Acknowledgment

We wish to thank Dr. U. Handge (Helmholtz-Zentrum Geesthacht) for stimulating discussions. Previous investigations in this field were supported by DGMK.

Appendix A. Supplementary data

Supplementary data associated with this article can be found, in the online version, at http://dx.doi.org/10.1016/j.carbpol.2014.11.050.

References

Baar, A., Kulicke, W.-M., Szablikowski, K., & Kiesewetter, R. (1994). Nuclear magnetic resonance spectroscopic characterization of carboxymethylcellulose. *Macromolecular Chemistry and Physics*, *195*, 1483–1492.

Bahamdan, A., & Daly, W. H. (2007). Hydrophobic guar gum derivatives prepared by controlled grafting processes—Part II: Rheological and degradation properties toward fracturing fluids applications. *Polymers for Advanced Technologies*, *18*, 660–672.

Banerjee, P., Mukherjee, I., Bhattacharya, S., Datta, S., Moulik, S. P., & Sarkar, D. (2009). Sorption of water vapor, hydration, and viscosity of carboxymethylhydroxypropyl guar, diutan, and xanthan gums, and their molecular association with and without salts (NaCl $CaCl_2$, HCOOK, CH_3COONa, $(NH_4)_2SO_4$ and $MgSO_4$) in aqueous solution. *Langmuir*, *25*, 11647–11656.

Beer, M. U., Wood, P. J., & Weisz, J. (1999). A simple and rapid method for evaluation of Mark–Houwink–Sakurada constants of linear random coil polysaccharides using molecular weight and intrinsic viscosity determinated by high performance size exclusion chromatography: Application to guar galactomannan. *Carbohydrate Polymers*, *39*, 377–380.

Bouldin, M., Kulicke, W.-M., & Kehler, H. (1988). Prediction of the non-Newtonian viscosity and shear stability of polymer solutions. *Colloid and Polymer Science*, *266*, 793–805.

Büche, F. (1952). Viscosity self-diffusion, and allied effects in solid polymers. *Journal of Chemical Physics*, *20*, 1959–1964.

Cheng, Y., & Prud'homme, R. K. (2000). Enzymatic degradation of guar und substituted guar galactomannans. *Biomacromolecules*, *1*, 782–788.

Cheng, Y., Brown, K. M., & Prud'homme, R. K. (2002). Characterization and intermolecular interactions of hydroxypropyl guar solutions. *Biomacromolecules*, *3*, 456–461.

Clasen, C., & Kulicke, W.-M. (2001). Determination of viscoelastic and rheo-optical material functions of water-soluble cellulose derivatives. *Progress in Polymer Science*, *26*, 1839–1919.

Cox, W. P., & Merz, E. H. (1958). Correlation of dynamic and steady flow viscosities. *Journal of Polymer Science*, *28*, 619–622.

Dea, I. C. M., & Morrison, A. (1975). Chemistry interactions of seed galactomannans. *Advances in Carbohydrate Chemistry and Biochemistry*, *31*, 241–312.

Flory, P. J., & Fox, T. G. (1951). Treatment of intrinsic viscosities. *Journal of the American Chemical Society*, *73*, 1904–1908.

Goycoolea, F. M., Morris, E. R., & Gidley, M. J. (1995). Viscosity of galactomannans at alkaline and neutral pH: Evidence of 'hyperentanglement' in solution. *Carbohydrate Polymers*, *27*, 69–71.

Graessley, W. W., Hazelton, R. L., & Lindeman, L. R. (1967). The shear-rate dependence of viscosity in concentrated solutions of narrow-distribution polystryene. *Transactions of The Society of Rheology*, *11*, 267–285.

Hoffman, J., & Svensson, S. (1978). Studies of the distribution of the D-galactosyl side-chains in guaran. *Carbohydrate Research*, *65*, 65–71.

Kesevan, S., & Prud'homme, R. K. (1992). Rheology of guar and HPG cross-linked by borate. *Macromolecules*, *25*, 2026–2032.

Kulicke, W.-M., & Klare, J. (1980). Eine η-*c*-*M*-Beziehung für polymerlösungen. *Die Angewandte Makromolekulare Chemie*, *84*, 67–79.

Kulicke, W.-M., & Kniewske, R. (1984). The shear viscosity dependence on concentration, molecular weight, and shear rate of polystyrene solutions. *Rheologica Acta*, *23*, 75–83.

Kulicke, W.-M., Kniewske, R., Müller, R.-J., Prescher, M., & Kehler, H. (1986). Scherung und degradation von polymerlösungen. *Die Angewandte Makromolekulare Chemie*, *142*, 29–49.

Kulicke, W.-M., Otto, M., & Baar, A. (1993). Improved NMR characterization of high-molecular-weight polymers and polyelectrolytes through the use of preliminary ultrasonic degradation. *Die Makromolekulare Chemie*, *194*, 751–765.

Kulicke, W.-M., & Clasen, C. (2004). *Viscosimetry of polymers and polyelectrolytes*. Berlin: Springer.

Lapasin, R., De Lorenzi, L., Pricl, S., & Torriano, G. (1995). Flow properties of hydroxypropyl guar gum and its long-chain hydrophobic derivatives. *Carbohydrate Polymers*, *27*, 195–202.

Laun, H. M. (1986). Prediction of elastic strains of polymer melts in shear and elongation. *Journal of Rheology*, *30*, 459.

Lei, C., & Clark, P. E. (2007). Crosslinking of guar and guar derivatives. *SPE Journal*, *12*, 316–321.

Ma, X., & Pawlik, M. (2007). Intrinsic viscosities and huggins constants of guar gum in alaki metal chloride solutions. *Carbohydrate Polymers*, *70*, 15–24.

McCleary, B. V., Clark, A. H., Dea, I. C. M., & Rees, D. A. (1985). The fine structures of carob and guar galactomannans. *Carbohydrate Research*, *139*, 237–260.

Morris, E. R., Cutler, A. N., Ross-Murphy, S. B., Rees, D. A., & Price, J. (1981). Concentration and shear rate dependence of viscosity in random coil polysaccharide solutions. *Carbohydrate Polymers*, *1*, 5–21.

Mukherjee, I., Sarkar, D., & Moulik, S. P. (2010). Interaction of gums (guar, carboxymethylhydroxypropyl guar, diutan, and xanthan) with surfactants (DTAB, CTAB and TX-100) in aqueous medium. *Langmuir*, *26*, 17906–17912.

Pasha, M., & Ngn, S. (2008). Derivatization of guar to sodium carboxymethyl hydroxypropyl derivative: Characterization and evaluation. *Pakistan Journal of Pharmaceutical Sciences*, *21*, 40–44.

Picout, D. R., Ross-Murphy, S. B., Errington, N., & Harding, S. E. (2001). Pressure cell assisted solution characterization of polysaccharides. 1. Guar gum. *Biomacromolecules*, *2*, 1301–1309.

Risica, D., Dentini, M., & Crescenzi, V. (2005). Guar gum methyl ethers. Part I. Synthesis and macromolecular characterization. *Polymer*, *46*, 12247–12255.

Risica, D., Barbetta, A., Vishetti, L., Cametti, C., & Dentini, M. (2010). Rheological properties of guar and its methyl, hydroxypropyl and hydroxypropyl-methyl derivatives in semidilute and concentrated aqueous solutions. *Polymer*, *51*, 1972–1982.

Robinson, G., Ross-Murphy, S. B., & Morris, E. R. (1982). Viscosity–molecular weight relationships, intrinsic chain flexibility, and dynamic solution properties of guar galactomannan. *Carbohydrate Research*, *107*, 17–32.

Sharma, V., & McKinley, G. H. (2012). An intriguing empirical rule for computing the first normal stress difference from steady shear viscosity data for polymer solutions and melts. *Rheologica Acta*, *51*, 487–495.

Shi, H.-Y., & Zhang, L.-M. (2007). New grafted polysaccharides based on *O*-carboxymethyl-*O*-hydroxypropyl guar gum and *N*-isopropylacrylamide: Synthesis and phase transition behavior in aqueous media. *Carbohydrate Polymers*, *67*, 337–342.

Simha, R., & Zakin, J. L. (1962). Solution viscosities of linear flexible high polymers. *Journal of Colloid Science*, *17*, 270–287.

Stockmayer, W. H., & Fixman, M. (1963). On the estimation of unperturbed dimensions from intrinsic viscosities. *Journal of Polymer Science, C: Polymer Symposia*, *1*, 137.

Storz, H., Zimmermann, U., Zimmermann, H., & Kulicke, W.-M. (2010). Viscoelastic properties of ultra-high viscosity alginates. *Rheologica Acta*, *49*, 155–167.

Tayal, A., Pai, V. B., & Khan, S. A. (1999). Rheology and molecular weight changes during enzymatic degradation of a water-soluble polymer. *Macromolecules*, *32*, 5567–5574.

Thielking, H., & Kulicke, W.-M. (1996). On-line coupling of flow field-flow fractionation and multiangle laser light scattering for the characterization of macromolecules in aqueou. *Analytical Chemistry*, *68*, 1169–1173.

Tizzotti, M., Labeau, M.-P., Hamaide, T., Drockenmuller, E., Charlot, A., & Fleury, E. (2010). Synthesis of thermosensitive guar-based hydrogels with tunable physico-chemical properties by click chemistry. *Journal of Polymer Science, A: Polymer Chemistry*, *48*, 2733–2742.

Venkataiah, S., & Mahadevan, E. G. (1982). Rheological properties of hydroxypropyl- and sodium carboxymethyl-substituted guar gums in aqueous solution. *Journal of Applied Polymer Science*, *27*, 1533–1548.

Vijayendran, B. R., & Bone, T. (1984). Absolute molecular weight und molecular weight distribution of guar by size exclusion chromatography and low-angle laser light scattering. *Carbohydrate Polymers*, *4*, 299–313.

Wientjes, R. H. W., Duits, M. H. G., Jongschaap, R. J. J., & Mellema, J. (2000). Linear rheology of guar gum solutions. *Macromolecules*, *33*(26), 9594–9605.

Yamakawa, H. (1971). *Modern theory of polymer solutions*. New York, NY: Harper and Row.

Yasuda, K., Armstrong, R. C., & Cohen, R. E. (1981). Shear flow properties of concentrated solutions of linear and star branched polystyrenes. *Rheologica Acta*, *20*, 163.

Yasuda, K. (2006). A multi-mode viscosity model and its applicability to non-newtonian fluids. *Journal of Textile Engineering*, *52*, 171–173.

Zhang, L.-M., Zhou, J.-F., & Hui, P. S. (2005). A comparative study on the viscosity behavior of water-soluble chemically modified guar gum derivatives with different functional lateral groups. *Journal of the Science of Food and Agriculture*, *85*, 2638–2644.

Zhang, L.-M., & Zhou, J.-F. (2006). Synergistic viscosity characteristics of aqueous mixed solutions of hydroxypropyl- and carboxymethyl-substituted guar gums. *Colloids and Surfaces, A: Physicocehmical and Engineering Aspects*, *279*, 34–39.